NUWC-NPT Technical Report 11,904
11 January 2010

A Dynamic Model of an Axisymmetric, Transversely Isotropic, Fluid-Loaded, Fully Elastic Cylindrical Shell

Andrew J. Hull
Autonomous and Defensive Systems Department

NAVSEA
WARFARE CENTERS
NEWPORT

Naval Undersea Warfare Center Division
Newport, Rhode Island

PREFACE

This report was prepared under Program Element 060274N, Project No. 04708, “Acoustic Vector Sensing,” principal investigator Kimberly M. Cipolla (Code 1512). The sponsoring activity is the Office of Naval Research (Michael Traweek, ONR-321).

The technical reviewer for this report was Jason M. Maguire (Code 1512).

The author thanks ONR program officer Michael Traweek for sponsorship of this work.

Reviewed and Approved: 11 January 2010

James S. Griffin
Head, Autonomous and Defensive Systems Department

REPORT DOCUMENTATION PAGE			*Form Approved* *OMB No. 0704-0188*

1. REPORT DATE (*DD-MM-YYYY*)	2. REPORT TYPE	3. DATES COVERED (*From – To*)
11-01-2010	Interim	

4. TITLE AND SUBTITLE A Dynamic Model of an Axisymmetric, Transversely Isotropic, Fluid-Loaded, Fully Elastic Cylindrical Shell	**5a. CONTRACT NUMBER** **5b. GRANT NUMBER** **5c. PROGRAM ELEMENT NUMBER** 060274N
6. AUTHOR(S) Andrew J. Hull	**5. d PROJECT NUMBER** 04708 **5e. TASK NUMBER** **5f. WORK UNIT NUMBER**
7. PERFORMING ORGANIZATION NAME(S) AND ADDRESS(ES) Naval Undersea Warfare Center Division 1176 Howell Street Newport, RI 02841-1708	**8. PERFORMING ORGANIZATION REPORT NUMBER** TR 11,904
9. SPONSORING/MONITORING AGENCY NAME(S) AND ADDRESS(ES) Office of Naval Research 875 North Randolph Street Suite 1425 Arlington VA 22203-1995	**10. SPONSORING/MONITOR'S ACRONYM** ONR **11. SPONSORING/MONITORING REPORT NUMBER**

12. DISTRIBUTION/AVAILABILITY STATEMENT

Approved for public release; distribution is unlimited.

13. SUPPLEMENTARY NOTES

20100408130

14. ABSTRACT

A fully elastic model of a transversely isotropic, fluid-loaded cylindrical shell is derived. The model is based on transversely isotropic equations of motion in the cylindrical coordinate system. Using the radial and longitudinal equations of motion, two free wavenumbers of the shell are determined, allowing the displacement field of the shell to be written as a linear expression with four unknown wave propagation coefficients. These displacements are used in the stress boundary conditions, where the fluid loading and the external forcing are added to the model. This produces a four-by-four system of equations that can be solved to obtain a solution to the wave propagation coefficients. This solution gives a known displacement field, a known inner pressure field, and a known outer pressure field. The model is validated using two previously derived shell models. An example is included to illustrate the model output where the specific interest is on the transfer function of inner pressure divided by external radial pressure and inner pressure divided by external longitudinal pressure. Finally, the MATLAB code used to generate this model is included for future use.

15. SUBJECT TERMS

Elastic Cylindrical Shells   Elastic Theory   Fluid-Loaded Shells   Shell Theory

16. SECURITY CLASSIFICATION OF:			17. LIMITATION OF ABSTRACT	18. NUMBER OF PAGES	19a. NAME OF RESPONSIBLE PERSON
a. REPORT	b. ABSTRACT	c. THIS PAGE			Andrew J. Hull
(U)	(U)	(U)	SAR	43	19b. TELEPHONE NUMBER (*Include area code*) (401) 832-5189

Standard Form 298 (Rev. 8-98)
Prescribed by ANSI Std. Z39-18

TABLE OF CONTENTS

LIST OF ILLUSTRATIONS

LIST OF ILLUSTRATIONS (Cont'd)

A DYNAMIC MODEL OF AN AXISYMMETRIC, TRANSVERSELY ISOTROPIC, FLUID-LOADED, FULLY ELASTIC CYLINDRICAL SHELL

1. INTRODUCTION

Fluid-loaded shells are encountered in numerous natural and man-made applications. Examples include arteries, inner ear tubes, hydraulic lines, marine pilings, water pipes, and shock absorbers. Understanding the behavior of these systems is important so that their performance can be analyzed or, in the case of mechanical systems, the next generation can be better designed. Extensive modeling of these systems has been done over the years, and a large volume of research articles exists in the area of cylindrical and spherical shells. From a complexity standpoint, membrane models of shells are the most simplistic and have been derived and analyzed most notably by Love.[1] A bending stiffness term was added to the membrane equations by Donnell.[2] Rotary inertia and shear effects were added to the cylindrical shell equations by Mirsky and Herrmann.[3,4] These previous models are based on membrane and flexural wave theory and are accurate only at low frequencies and low wavenumbers. The fully elastic, isotropic cylindrical shell was modeled and analyzed by Gazis.[5,6] The work by Gazis was a significant extension of previous theory as it allowed analytical modeling at all frequencies and wavenumbers, rather than just a small subset of low-frequency and low-wavenumber analysis. The fully elastic, transversely isotropic cylindrical shell was modeled by Laverty[7] for analysis of wood cylinders. Fay[8] added fluid loading to the membrane theories for a solid cylinder. Additionally, Peloquin[9] added fluid loading to various flexural wave theories for hollow cylinders.

This report develops an analytical model of a transversely isotropic, fluid-loaded, fully elastic axisymmetric cylinder that is in contact with fluid on both its interior and exterior. The model begins with the equations of motion of a transversely isotropic body in cylindrical coordinates. Using the radial and longitudinal equations of motion, two free wavenumbers are calculated corresponding to two specific waves that are propagating in the medium. A solution set to the shell displacement field is formulated that contains four unknown wave propagation coefficients. These coefficients are inserted into the stress boundary conditions at the inner and outer surfaces of the shell. Also included in these boundary conditions are the pressure loads of the inner and outer fluid fields and any external loads that may be acting on the system. This produces four algebraic equations with four unknown wave propagation coefficients. This set of equations can be solved to obtain an analytical solution to the shell displacements, the pressure of the inner fluid, and the pressure of the outer fluid. The model is verified by comparing the results with two previously derived models, and a numerical example is included to illustrate the behavior of a thick shell under two loading conditions. Additionally, a MATLAB subroutine is included that contains a vectorized computation that outputs interior shell pressure produced from external forcing functions.

2. SYSTEM MODEL

The system equations consist of three separate models: the cylindrical shell equations of motion in the radial and axial direction, the inner acoustic field wave equation of pressure, and the outer acoustic field wave equation of pressure. Once the general solutions to these equations of motions and pressure are determined, they are coupled using linear momentum and inserted into the stress fields at the inner and outer radii of the shell. This produces a four-by-four matrix that contains the dynamics of the system multiplied by a four-by-one vector that contains the unknown wave propagation coefficients and is equal to a four-by-one vector containing the applied external loads. This matrix equation can be solved and the response of the system can be calculated. This process is described below. A schematic of the system illustrating the coordinate system is shown in figure 1.

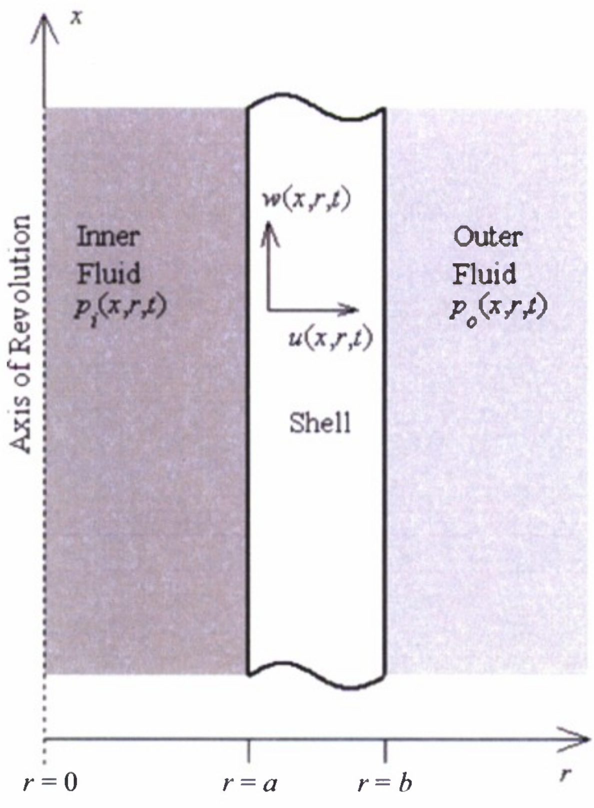

Figure 1. Fluid-Loaded Shell with Coordinate System

The equation of motion of a fully elastic, isotropic body in cylindrical coordinates[10] in the radial direction is

$$\rho\frac{\partial^2 u(x,r,t)}{\partial t^2}=c_{11}\left[\frac{\partial^2 u(x,r,t)}{\partial r^2}+\frac{1}{r}\frac{\partial u(x,r,t)}{\partial r}-\frac{u(x,r,t)}{r^2}\right]+c_{44}\frac{\partial^2 u(x,r,t)}{\partial x^2}$$
$$+(c_{13}+c_{44})\frac{\partial^2 w(x,r,t)}{\partial r\partial x}, \tag{1}$$

in the longitudinal direction, the equation is

$$\rho\frac{\partial^2 w(x,r,t)}{\partial t^2}=(c_{13}+c_{44})\left[\frac{\partial^2 u(x,r,t)}{\partial r\partial x}+\frac{1}{r}\frac{\partial u(x,r,t)}{\partial x}\right]$$
$$+c_{44}\left[\frac{\partial^2 w(x,r,t)}{\partial r^2}+\frac{1}{r}\frac{\partial w(x,r,t)}{\partial r}\right]+c_{33}\frac{\partial^2 w(x,r,t)}{\partial x^2}\quad . \tag{2}$$

In equations (1) and (2), $u(x,r,t)$ is the displacement in the radial direction (m), $w(x,r,t)$ is the displacement in the longitudinal direction (m), r is the coordinate of the radial direction (m), x is the coordinate of the longitudinal direction (m), t is time (s), ρ is density of the shell (kg m^{-3}), and c_{ij} are stiffness constants that contain the material properties (N m^{-2}) and are typically complex quantities. These constants are determined using the constitutive equations in cylindrical coordinates between strain and stress written for a solid that is transversely isotropic in the axial direction with respect to the radial and circumferential directions. These equations are

$$\varepsilon_{rr}=\frac{1}{E_r}\sigma_{rr}-\frac{\upsilon_{rx}}{E_r}\sigma_{\theta\theta}-\frac{\upsilon_{xr}}{E_x}\sigma_{xx}\ , \tag{3}$$

$$\varepsilon_{\theta\theta}=-\frac{\upsilon_{rx}}{E_r}\sigma_{rr}+\frac{1}{E_r}\sigma_{\theta\theta}-\frac{\upsilon_{xr}}{E_x}\sigma_{xx}\ , \tag{4}$$

$$\varepsilon_{xx}=-\frac{\upsilon_{rx}}{E_r}\sigma_{rr}-\frac{\upsilon_{rx}}{E_r}\sigma_{\theta\theta}+\frac{1}{E_x}\sigma_{xx}\ , \tag{5}$$

$$\gamma_{x\theta}=\frac{1}{G_{xr}}\tau_{x\theta}\ , \tag{6}$$

$$\gamma_{xr} = \frac{1}{G_{xr}} \tau_{xr} , \tag{7}$$

and

$$\gamma_{x\theta} = \frac{1}{G_{rx}} \tau_{r\theta} , \tag{8}$$

where ε_{ii} are the normal strains (dimensionless), γ_{ij} are the shear strains (dimensionless), σ_{ii} are the normal stresses (N m^{-2}), τ_{ij} are the shear stresses (N m^{-2}), E_r is Young's modulus in the radial direction (N m^{-2}), E_x is Young's modulus in the axial direction (N m^{-2}), υ_{rx} is Poisson's ratio in the longitudinal direction with a load being applied in the radial direction (dimensionless), and υ_{xr} is Poisson's ratio in the radial direction with a load being applied in the longitudinal direction (dimensionless). Equations (3) through (8) are inverted so that the stresses are functions of the strains, which in matrix form is

$$\boldsymbol{\sigma} = \mathbf{C}\boldsymbol{\varepsilon} , \tag{9}$$

where

$$\boldsymbol{\sigma} = \begin{bmatrix} \sigma_{rr} & \sigma_{\theta\theta} & \sigma_{xx} & \tau_{x\theta} & \tau_{xr} & \tau_{r\theta} \end{bmatrix}^{\mathrm{T}} , \tag{10}$$

and

$$\boldsymbol{\varepsilon} = \begin{bmatrix} \varepsilon_{rr} & \varepsilon_{\theta\theta} & \varepsilon_{xx} & \gamma_{x\theta} & \gamma_{xr} & \gamma_{r\theta} \end{bmatrix}^{\mathrm{T}} . \tag{11}$$

Using equation (9) and Betti's reciprocal law for composite materials, written as

$$\frac{\upsilon_{rx}}{E_r} = \frac{\upsilon_{xr}}{E_x} , \tag{12}$$

the stiffness constants in equations (1) and (2) can be solved for in terms of engineering constants. They are

$$c_{11} = \frac{E_r(1 - \upsilon_{rx}\upsilon_{xr})}{(1 + \upsilon_{rx})(1 - \upsilon_{rx} - 2\upsilon_{rx}\upsilon_{xr})} , \tag{13}$$

$$c_{12} = \frac{E_r \upsilon_{rx}(1+\upsilon_{xr})}{(1+\upsilon_{rx})(1-\upsilon_{rx}-2\upsilon_{rx}\upsilon_{xr})}, \tag{14}$$

$$c_{13} = \frac{E_r \upsilon_{xr}}{(1-\upsilon_{rx}-2\upsilon_{rx}\upsilon_{xr})}, \tag{15}$$

$$c_{33} = \frac{E_r \upsilon_{xr}(1-\upsilon_{rx})}{\upsilon_{rx}(1-\upsilon_{rx}-2\upsilon_{rx}\upsilon_{xr})}, \tag{16}$$

and

$$c_{44} = G_{xr} = \frac{E_x}{2(1+\upsilon_{xr})}. \tag{17}$$

The solution to equations (1) and (2) is now determined for free wave propagation in a medium that is bounded in the radial direction, unbounded in the axial direction, and harmonic in time. The argument is made[7] that the solution to the transversely isotropic differential equations has to have the same form as the solution to the isotropic differential equations. Thus, the solution in the radial direction is written as

$$u(r,x,t) = U(r)\exp(\mathrm{i}kx)\exp(-\mathrm{i}\omega t) = G\mathrm{B}_1(\gamma r)\exp(\mathrm{i}kx)\exp(-\mathrm{i}\omega t), \tag{18}$$

and the solution in the longitudinal direction is written as

$$w(r,x,t) = W(r)\exp(\mathrm{i}kx)\exp(-\mathrm{i}\omega t) = H\mathrm{B}_0(\gamma r)\exp(\mathrm{i}kx)\exp(-\mathrm{i}\omega t), \tag{19}$$

where G and H are unknown wave propagation coefficients, B_1 denotes an ordinary Bessel function of order one, B_0 denotes an ordinary Bessel function of order zero, γ is the free propagation wavenumber (rad m^{-1}), k is the wavenumber with respect to the x-axis (rad m^{-1}), and i is $\sqrt{-1}$. It is noted that the free propagation wavenumbers are typically complex quantities; thus, the Bessel functions contain complex arguments. To facilitate this type of analysis, the Bessel functions will all be ordinary Bessel functions of the first and second kind with complex arguments, rather than switching between normal and modified Bessel functions based on the sign of the argument. Substituting equations (18) and (19) into equations (1) and (2) yields the two-by-two system of algebraic equations, written as

$$\begin{bmatrix} \rho\omega^2 - c_{11}\gamma^2 - c_{44}k^2 & -ik\gamma(c_{13}+c_{44}) \\ ik\gamma(c_{13}+c_{44}) & \rho\omega^2 - c_{44}\gamma^2 - c_{33}k^2 \end{bmatrix} \begin{Bmatrix} G \\ H \end{Bmatrix} = \begin{Bmatrix} 0 \\ 0 \end{Bmatrix} . \tag{20}$$

The determinant of the two-by-two matrix in equation (20) must be zero if a solution other than the trivial solution is going to exist. This yields a quadratic equation with respect to the propagation wavenumber γ^2 that is written as

$$a\gamma^4 + b\gamma^2 + c = 0 , \tag{21}$$

where

$$a = c_{11}c_{44} , \tag{22}$$

$$b = (c_{11}c_{33} - c_{13}^2 - 2c_{13}c_{44})k^2 - (c_{44} + c_{11})\rho\omega^2 , \tag{23}$$

and

$$c = \rho^2\omega^4 - (c_{33} + c_{44})\rho\omega^2 k^2 + c_{33}c_{44}k^4 . \tag{24}$$

The solution to equation (21) is

$$\gamma_{1,2} = \left[\frac{-b \pm (b^2 - 4ac)^{1/2}}{2a} \right]^{1/2} . \tag{25}$$

Only the positive values from equation (25) are needed, as the zero-order and first-order Bessel functions in equations (18) and (19) are even functions; thus, negative values will not contribute to a linearly independent solution. The first row of equation (20) yields

$$\begin{aligned} H &= \frac{\rho\omega^2 - c_{11}\gamma^2 - c_{44}k^2}{ik\gamma_{1,2}(c_{13}+c_{44})} G \\ &= \xi_{1,2} G . \end{aligned} \tag{26}$$

The solution is now written as Bessel functions of the first kind using the wavenumbers γ_1 and γ_2. The expressions for the displacement fields are

$$u(x,r,t) = [G_1 \mathrm{J}_1(\gamma_1 r) + G_3 \mathrm{J}_1(\gamma_2 r)]\exp(\mathrm{i}kx)\exp(-\mathrm{i}\omega t)\,, \tag{27}$$

and

$$\begin{aligned} w(x,r,t) &= [H_1 \mathrm{J}_0(\gamma_1 r) + H_3 \mathrm{J}_0(\gamma_2 r)]\exp(\mathrm{i}kx)\exp(-\mathrm{i}\omega t) \\ &= [G_1 \xi_1 \mathrm{J}_0(\gamma_1 r) + G_3 \xi_2 \mathrm{J}_0(\gamma_2 r)]\exp(\mathrm{i}kx)\exp(-\mathrm{i}\omega t)\,. \end{aligned} \tag{28}$$

Additionally, because the domain of r is from $a(>0)$ to $b(<\infty)$, Bessel functions of the second kind are admissible solutions, and the expressions for the displacement fields using these functions are

$$u(x,r,t) = [G_2 \mathrm{Y}_1(\gamma_1 r) + G_4 \mathrm{Y}_1(\gamma_2 r)]\exp(\mathrm{i}kx)\exp(-\mathrm{i}\omega t)\,, \tag{29}$$

and

$$\begin{aligned} w(x,r,t) &= [H_2 \mathrm{Y}_0(\gamma_1 r) + H_4 \mathrm{Y}_0(\gamma_2 r)]\exp(\mathrm{i}kx)\exp(-\mathrm{i}\omega t) \\ &= [G_2 \xi_1 \mathrm{Y}_0(\gamma_1 r) + G_4 \xi_2 \mathrm{Y}_0(\gamma_2 r)]\exp(\mathrm{i}kx)\exp(-\mathrm{i}\omega t)\,. \end{aligned} \tag{30}$$

The problem set represented by equations (27) and (28) is linearly independent from the solution set given by equations (29) and (30), and a complete solution is a linear combination of both equation sets. This gives the total solution to the shell displacements as

$$u(x,r,t) = [G_1 \mathrm{J}_1(\gamma_1 r) + G_2 \mathrm{Y}_1(\gamma_1 r) + G_3 \mathrm{J}_1(\gamma_2 r) + G_4 \mathrm{Y}_1(\gamma_2 r)]\exp(\mathrm{i}kx)\exp(-\mathrm{i}\omega t)\,, \tag{31}$$

and

$$w(x,r,t) = [G_1 \xi_1 \mathrm{J}_0(\gamma_1 r) + G_2 \xi_1 \mathrm{Y}_0(\gamma_1 r) + G_3 \xi_2 \mathrm{J}_0(\gamma_2 r) + G_4 \xi_2 \mathrm{Y}_0(\gamma_2 r)]\exp(\mathrm{i}kx)\exp(-\mathrm{i}\omega t)\,, \tag{32}$$

where G_1, G_2, G_3, and G_4 are unknown wave propagation coefficients. The insertion of equations (31) and (32) into equations (1) and (2) verifies that they are solutions to the original differential equations of motion.

The unknown wave propagation coefficients are determined using the four stress-boundary conditions of the shell. The first boundary condition is a force balance between the pressure in the interior fluid and the normal radial stress in the shell at the interface where $r = a$. This equation is written as

$$\sigma_{rr}(x,a,t) = c_{11}\frac{\partial u(x,a,t)}{\partial r} + c_{12}\frac{u(x,a,t)}{a} + c_{13}\frac{\partial w(x,a,t)}{\partial x} = -p_i(x,a,t)\,, \tag{33}$$

where $p_i(x,a,t)$ is the pressure of the interior fluid (N m^{-2}) at $r = a$, which satisfies the wave equation in cylindrical coordinates; i.e.,

$$\frac{\partial^2 p_i(x,r,t)}{\partial r^2} + \frac{1}{r}\frac{\partial p_i(x,r,t)}{\partial r} + \frac{\partial^2 p_i(x,r,t)}{\partial x^2} - \frac{1}{c_i^2}\frac{\partial^2 p_i(x,r,t)}{\partial t^2} = 0\,, \tag{34}$$

where c_i is the acoustic (or compressional) wavespeed of the interior fluid (m s^{-1}). Using the infinite length of the cylinder in the x-direction and the constraint that the pressure field has to be finite at $r = 0$, the temporal harmonic solution to equation (34) is

$$p_i(x,r,t) = P_i(r)\exp(ikx)\exp(-i\omega t) = MJ_0(\gamma_i r)\exp(ikx)\exp(-i\omega t)\,, \tag{35}$$

where

$$\gamma_i = \left[\left(\frac{\omega}{c_i}\right)^2 - k^2\right]^{1/2} = (k_i^2 - k^2)^{1/2}\ . \tag{36}$$

In general, γ_i can be a complex quantity if the internal fluid acoustic wavespeed is complex; i.e., contains a loss term as an imaginary quantity. If the loss factor is zero, then the internal fluid acoustic wavespeed is purely real, and γ_i will be either purely real or purely imaginary. To relate the internal acoustic pressure field to the radial shell displacement field, conservation of momentum is invoked at the interface. This equation is

$$\rho_i \frac{\partial^2 u(x,a,t)}{\partial t^2} = -\frac{\partial p_i(x,a,t)}{\partial r} \; , \tag{37}$$

where ρ_i is the density of the interior fluid (kg m^{-3}). Inserting equations (31) and (35) into equation (37) allows the constant M to be determined and the pressure field to be written as

$$P_i(r) = \frac{-\omega^2 \rho_i}{\gamma_i} \frac{\mathrm{J}_0(\gamma_i r)}{\mathrm{J}_1(\gamma_i a)} [G_1 \mathrm{J}_1(\gamma_1 a) + G_2 \mathrm{Y}_1(\gamma_1 a) + G_3 \mathrm{J}_1(\gamma_2 a) + G_4 \mathrm{Y}_1(\gamma_2 a)] \; . \tag{38}$$

Inserting equations (31), (32), and (38) into equation (33) yields the first algebraic boundary value equation, written as

$$\begin{aligned}
&\left[(c_{11}\gamma_1 + ikc_{13}\xi_1)\mathrm{J}_0(\gamma_1 a) + \left(\frac{c_{12} - c_{11}}{a} + \frac{-\omega^2 \rho_i}{\gamma_i} \frac{\mathrm{J}_0(\gamma_i a)}{\mathrm{J}_1(\gamma_i a)} \right) \mathrm{J}_1(\gamma_1 a) \right] G_1 \\
&+ \left[(c_{11}\gamma_1 + ikc_{13}\xi_1)\mathrm{Y}_0(\gamma_1 a) + \left(\frac{c_{12} - c_{11}}{a} + \frac{-\omega^2 \rho_i}{\gamma_i} \frac{\mathrm{J}_0(\gamma_i a)}{\mathrm{J}_1(\gamma_i a)} \right) \mathrm{Y}_1(\gamma_1 a) \right] G_2 \\
&+ \left[(c_{11}\gamma_2 + ikc_{13}\xi_2)\mathrm{J}_0(\gamma_2 a) + \left(\frac{c_{12} - c_{11}}{a} + \frac{-\omega^2 \rho_i}{\gamma_i} \frac{\mathrm{J}_0(\gamma_i a)}{\mathrm{J}_1(\gamma_i a)} \right) \mathrm{J}_1(\gamma_2 a) \right] G_3 \\
&+ \left[(c_{11}\gamma_2 + ikc_{13}\xi_2)\mathrm{Y}_0(\gamma_2 a) + \left(\frac{c_{12} - c_{11}}{a} + \frac{-\omega^2 \rho_i}{\gamma_i} \frac{\mathrm{J}_0(\gamma_i a)}{\mathrm{J}_1(\gamma_i a)} \right) \mathrm{Y}_1(\gamma_2 a) \right] G_4 = 0 \, .
\end{aligned} \tag{39}$$

The second boundary condition is the radial-longitudinal shear stress in the shell at the interface where $r = a$ is zero, and this equation is written as

$$\sigma_{rx}(x,a,t) = c_{44} \left(\frac{\partial u(x,a,t)}{\partial x} + \frac{\partial w(x,a,t)}{\partial r} \right) = 0 \; . \tag{40}$$

Inserting equations (31) and (32) into equation (40) yields the second algebraic boundary value equation, written as

$$
\begin{aligned}
&[c_{44}(ik-\gamma_1\xi_1)\mathrm{J}_1(\gamma_1 a)]G_1 \\
&\quad+[c_{44}(ik-\gamma_1\xi_1)\mathrm{Y}_1(\gamma_1 a)]G_2 \\
&\quad+[c_{44}(ik-\gamma_2\xi_2)\mathrm{J}_1(\gamma_2 a)]G_3 \\
&\quad+[c_{44}(ik-\gamma_2\xi_2)\mathrm{Y}_1(\gamma_2 a)]G_4=0 .
\end{aligned}
\tag{41}
$$

The third boundary condition is a force balance between the pressure in the exterior fluid, an applied radial load, and the normal radial stress in the shell at the interface where $r = b$. This equation is written as

$$
\sigma_{rr}(x,b,t)=c_{11}\frac{\partial u(x,b,t)}{\partial r}+c_{12}\frac{u(x,b,t)}{b}+c_{13}\frac{\partial w(x,b,t)}{\partial x}=p_o(x,b,t)-p_e(x,t) \ , \tag{42}
$$

where $p_e(x,t)$ is an applied external forcing function (N m^{-2}) in the radial direction that is assumed to be at a discrete wavenumber and frequency; thus,

$$
p_e(x,t)=P_e\exp(\mathrm{i}kx)\exp(-\mathrm{i}\omega t) \ , \tag{43}
$$

and $p_o(x,b,t)$ is the scattered acoustic pressure of the exterior fluid (N m^{-2}) at $r = b$, which satisfies the wave equation in cylindrical coordinates; i.e.,

$$
\frac{\partial^2 p_o(x,r,t)}{\partial r^2}+\frac{1}{r}\frac{\partial p_o(x,r,t)}{\partial r}+\frac{\partial^2 p_o(x,r,t)}{\partial x^2}-\frac{1}{c_o^2}\frac{\partial^2 p_o(x,r,t)}{\partial t^2}=0 \ , \tag{44}
$$

where c_o is the acoustic (or compressional) wavespeed of the exterior fluid (m s^{-1}). Using the infinite length of the cylinder in the x-direction and the constraint that the pressure field has vanished when r approaches infinity, the temporal harmonic solution to equation (44) is

$$
p_o(x,r,t)=P_o(r)\exp(\mathrm{i}kx)\exp(-\mathrm{i}\omega t)=N\,\mathrm{H}_0^{(1)}(\gamma_o r)\exp(\mathrm{i}kx)\exp(-\mathrm{i}\omega t) \ , \tag{45}
$$

where $\mathrm{H}_0^{(1)}$ denotes a zero-order Hankel function of the first kind and

$$\gamma_o = \left[\left(\frac{\omega}{c_o} \right)^2 - k^2 \right]^{1/2} = (k_o^2 - k^2)^{1/2} \ . \tag{46}$$

The external fluid wavenumber γ_o can be a complex quantity if the external fluid acoustic wavespeed is complex, i.e., contains a loss term as an imaginary quantity. If the loss factor is zero, then the external fluid acoustic wavespeed is purely real, and γ_o will be either purely real or purely imaginary. To relate the external acoustic pressure field to the radial shell displacement field, conservation of momentum is invoked at the interface. This equation is

$$\rho_o \frac{\partial^2 u(x,b,t)}{\partial t^2} = -\frac{\partial p_o(x,b,t)}{\partial r} \ , \tag{47}$$

where ρ_o is the density of the exterior fluid (kg m^{-3}). Inserting equations (31) and (45) into equation (47) allows the constant N to be determined and the pressure field to be written as

$$P_o(r) = \frac{-\omega^2 \rho_o}{\gamma_o} \frac{\mathrm{H}_0^{(1)}(\gamma_o r)}{\mathrm{H}_1^{(1)}(\gamma_o a)} [G_1 \mathrm{J}_1(\gamma_1 b) + G_2 \mathrm{Y}_1(\gamma_1 b) + G_3 \mathrm{J}_1(\gamma_2 b) + G_4 \mathrm{Y}_1(\gamma_2 b)] \ . \tag{48}$$

Inserting equations (31), (32), and (48) into equation (42) yields the third algebraic boundary value equation, written as

$$\begin{aligned}
&\left[(c_{11}\gamma_1 + ikc_{13}\xi_1)\mathrm{J}_0(\gamma_1 b) + \left(\frac{c_{12} - c_{11}}{b} - \frac{-\omega^2 \rho_o}{\gamma_o} \frac{\mathrm{H}_0^{(1)}(\gamma_o b)}{\mathrm{H}_1^{(1)}(\gamma_o b)} \right) \mathrm{J}_1(\gamma_1 b) \right] G_1 \\
&+ \left[(c_{11}\gamma_1 + ikc_{13}\xi_1)\mathrm{Y}_0(\gamma_1 b) + \left(\frac{c_{12} - c_{11}}{b} - \frac{-\omega^2 \rho_o}{\gamma_o} \frac{\mathrm{H}_0^{(1)}(\gamma_o b)}{\mathrm{H}_1^{(1)}(\gamma_o b)} \right) \mathrm{Y}_1(\gamma_1 b) \right] G_2 \\
&+ \left[(c_{11}\gamma_2 + ikc_{13}\xi_2)\mathrm{J}_0(\gamma_2 b) + \left(\frac{c_{12} - c_{11}}{b} - \frac{-\omega^2 \rho_o}{\gamma_o} \frac{\mathrm{H}_0^{(1)}(\gamma_o b)}{\mathrm{H}_1^{(1)}(\gamma_o b)} \right) \mathrm{J}_1(\gamma_2 b) \right] G_3 \\
&+ \left[(c_{11}\gamma_2 + ikc_{13}\xi_2)\mathrm{Y}_0(\gamma_2 b) + \left(\frac{c_{12} - c_{11}}{b} - \frac{-\omega^2 \rho_o}{\gamma_o} \frac{\mathrm{H}_0^{(1)}(\gamma_o b)}{\mathrm{H}_1^{(1)}(\gamma_o b)} \right) \mathrm{Y}_1(\gamma_2 b) \right] G_4 = -P_e \ .
\end{aligned} \tag{49}$$

The fourth boundary condition is the radial-longitudinal shear stress in the shell at the interface where $r = b$ and is equal to an applied longitudinal load that is assumed to be at a discrete wavenumber and frequency; thus,

$$\sigma_{rx}(x,b,t) = c_{44}\left(\frac{\partial u(x,b,t)}{\partial x} + \frac{\partial w(x,b,t)}{\partial r}\right) = f_e(x,t), \tag{50}$$

where $f_e(x,t)$ is an applied external forcing function (N m^{-2}) in the longitudinal direction that is assumed to be at a discrete wavenumber and frequency; thus,

$$f_e(x,t) = F_e \exp(ikx)\exp(-i\omega t) \ . \tag{51}$$

Inserting equations (31), (32), and (51) into equation (50) yields the fourth algebraic boundary value equation, written as

$$\begin{aligned} &[c_{44}(ik - \gamma_1\xi_1)\mathrm{J}_1(\gamma_1 b)]G_1 \\ &\quad + [c_{44}(ik - \gamma_1\xi_1)\mathrm{Y}_1(\gamma_1 b)]G_2 \\ &\quad + [c_{44}(ik - \gamma_2\xi_2)\mathrm{J}_1(\gamma_2 b)]G_3 \\ &\quad + [c_{44}(ik - \gamma_2\xi_2)\mathrm{Y}_1(\gamma_2 b)]G_4 = F_e \ . \end{aligned} \tag{52}$$

Equations (39), (41), (49), and (52) are now written in matrix form as

$$\mathbf{Ag} = \mathbf{f} \ , \tag{53}$$

where $\mathbf{A}$ is a known four-by-four coefficient matrix, $\mathbf{g}$ is a four-by-one vector that contains the four unknown wave propagation coefficients, and $\mathbf{f}$ is a four-by-one load vector that represents the external forces exciting the system. (The entries of the matrix and vectors in equation (53) are given in appendix A.) The wave propagation coefficients are now found by

$$\mathbf{g} = \mathbf{A}^{-1}\mathbf{f} \ . \tag{54}$$

Once the wave propagation coefficients are known, the shell displacements can be calculated using equations (31) and (32), the exterior pressure field can be calculated using equation (48), and the interior pressure field can be calculated using equation (38).

3. MODEL VALIDATION

The model is now validated by comparison to previously developed shell theories. First, the fully elastic thick shell model derived in section 2 is compared to a transversely isotropic thin shell model. From a previously developed isotropic thin shell model,[11] fluid loading is added to produce a longitudinal equation of motion, written as

$$\rho h \frac{\partial^2 w(x,t)}{\partial t^2} = \frac{hE_x}{(1-\upsilon_{rx}\upsilon_{xr})} \frac{\partial^2 w(x,t)}{\partial x^2} + \frac{h\upsilon_{xr}E_r}{a(1-\upsilon_{rx}\upsilon_{xr})} \frac{\partial u(x,t)}{\partial x} + f_e(x,t) \ , \tag{55}$$

and a radial equation of motion, written as

$$\begin{aligned} \rho h \frac{\partial^2 u(x,t)}{\partial t^2} = -B \frac{\partial^4 u(x,t)}{\partial x^4} - \frac{hE_r}{a^2(1-\upsilon_{rx}\upsilon_{xr})} u(x,t) - \frac{h\upsilon_{rx}E_x}{a(1-\upsilon_{rx}\upsilon_{xr})} \frac{\partial w(x,t)}{\partial x}, \\ + p_i(a,x,t) - p_o(a,x,t) - p_e(x,t) , \end{aligned} \tag{56}$$

where B is the flexural stiffness (N m) of the shell and is given by

$$B = \frac{h^3 E_x}{12(1-\upsilon_{rx}\upsilon_{xr})} \ . \tag{57}$$

Making the assumption of harmonic response in space and time, the displacements can be written as

$$u(x,t) = U \exp(\mathrm{i}kx)\exp(\mathrm{i}\omega t) , \tag{58}$$

and

$$w(x,t) = W \exp(\mathrm{i}kx)\exp(\mathrm{i}\omega t) \ . \tag{59}$$

This produces the matrix equation

$$\mathbf{Bu} = \mathbf{p} \ , \tag{60}$$

where the unknown displacements are contained in the vector **u**. (The entries of the matrix and vectors in equation (60) are listed in appendix A.) The unknown displacements are determined using

$$\mathbf{u} = \mathbf{B}^{-1}\mathbf{p} \ . \tag{61}$$

Once the displacements are known, the interior pressure field for this model can be calculated using

$$P_i(r) = \frac{-\omega^2 \rho_i}{\gamma_i} \frac{\mathrm{J}_0(\gamma_i r)}{\mathrm{J}_1(\gamma_i a)} U \ , \tag{62}$$

and the exterior pressure filed can be calculated using

$$P_o(r) = \frac{-\omega^2 \rho_o}{\gamma_o} \frac{\mathrm{H}_0^{(1)}(\gamma_o r)}{\mathrm{H}_1^{(1)}(\gamma_o a)} U \ . \tag{63}$$

Figure 2 is a plot of the transfer function of internal pressure at $r = 0$ divided by external forcing function in the radial direction versus wavenumber. Figure 3 is a plot of the transfer function of internal pressure at $r = 0$ divided by external forcing function in the longitudinal direction versus wavenumber. In both figures, the upper plot is the magnitude of the power expressed in the decibel scale and the lower plot is the phase angle expressed in degrees. The solid line is the transversely isotropic thick shell model developed in section 2 and the dots correspond to the transversely isotropic thin shell model listed as equations (55) through (63). In this example, the thickness of the shell was small (5.08×10^{-4} m) and the frequency was low (100 Hz), so the assumptions of the thin shell model are valid and the outputs of the two models should reasonably agree. Figures 2 and 3 were generated with the following parameters: shell density $\rho = 1200$ kg m^{-3}, radial Poisson's ratio due to longitudinal load $\upsilon_{xr} = 0.48$ (dimensionless), longitudinal Young's modulus $E_x = 2 \times 10^9$ N m^{-2}, radial Young's modulus $E_r = 3 \times 10^8$ N m^{-2}, longitudinal Poisson's ratio due to radial load $\upsilon_{rx} = 0.072$ (dimensionless), shear modulus $G_{xr} = 6.76 \times 10^8$ N m^{-2}, inner shell radius $a = 0.0759$ m, outer shell radius $b = 0.0765$ m, inner fluid density $\rho_i = 800$ kg m^{-3}, inner fluid compressional wavespeed $c_i = 1300$ m s^{-1}, outer fluid density $\rho_o = 1000$ kg m^{-3}, and outer fluid compressional wavespeed $c_o = 1500$ m s^{-1}. Based on these values, the computed stiffness constants are $c_{11} = 3.15 \times 10^8$ N m^{-2}, $c_{12} = 3.47 \times 10^7$ N m^{-2}, $c_{13} = 1.68 \times 10^8$ N m^{-2}, $c_{33} = 2.16 \times 10^9$ N m^{-2}, and $c_{44} = 6.76 \times 10^8$ N m^{-2}. For the model validation problems presented here, the shell has zero damping; however, most structures have some loss mechanism associated with their behavior.

Note that in figures 2 and 3, there is broad-based agreement between the thin shell model and the thick shell model. It is noted that these two transfer functions are of interest, and these specific outputs will be investigated in the remainder of this report.

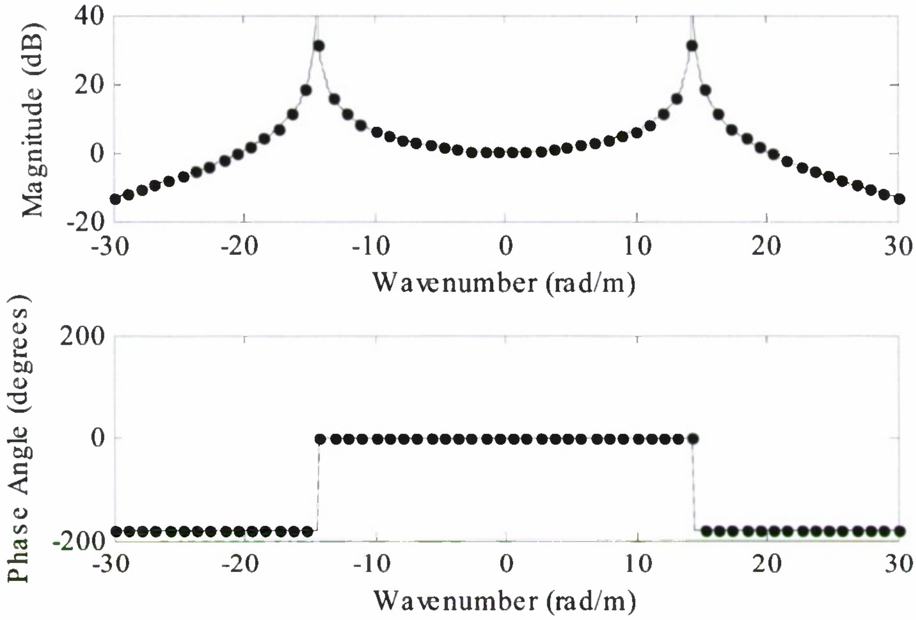

Figure 2. Transfer Function of Internal Pressure Divided by External Radial Excitation: Transversely Isotropic Thick Shell (——) and Transversely Isotropic Thin Shell (•)

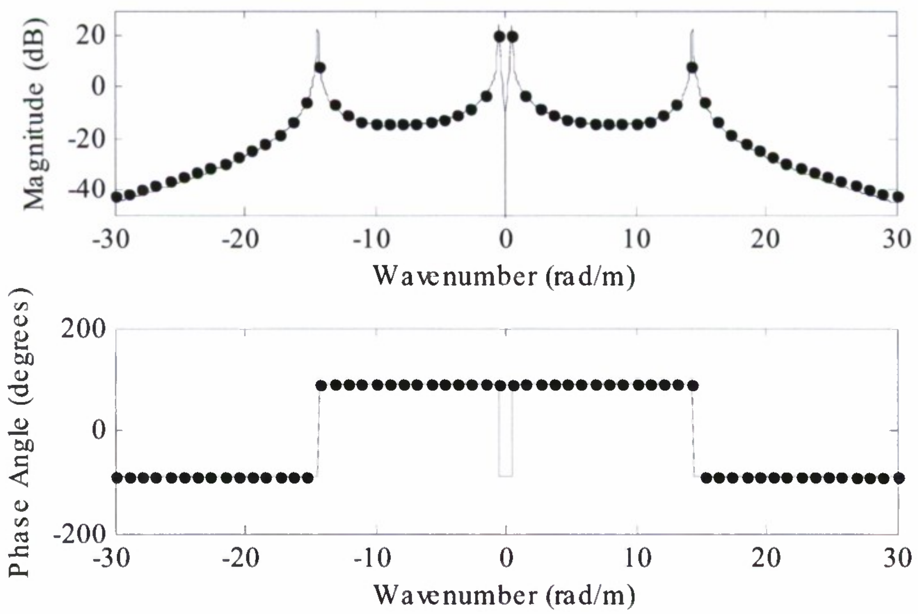

Figure 3. Transfer Function of Internal Pressure Divided by External Longitudinal Excitation: Transversely Isotropic Thick Shell (——) and Transversely Isotropic Thin Shell (•)

Next, the fully elastic thick shell model derived in section 2 is compared to a fully elastic isotropic thick shell model. A previously developed thick shell model[5,6] is based on Navier's equation of motion in an isotropic solid, written in vector form as

$$(\lambda+\mu)\nabla\nabla \bullet \mathbf{u}+\mu\nabla^2\mathbf{u}=\rho\frac{\partial^2\mathbf{u}}{\partial t^2} \ , \tag{64}$$

where λ and μ are Lamé constants (N m^{-2}) of the shell and the vector $\mathbf{u}$ represents the displacement field (m). This equation is solved and coupled to the inner and outer pressure field and the result is the matrix equation

$$\mathbf{Cd}=\mathbf{f} \ , \tag{65}$$

where $\mathbf{C}$ is a known four-by-four coefficient matrix, $\mathbf{d}$ is a four-by-one vector that contains four unknown wave propagation coefficients, and $\mathbf{f}$ is a four-by-one load vector that represents the external forces exciting the system. (The entries of the matrix and vectors in equation (65) are given in appendix A.) The wave propagation coefficients are now found by

$$\mathbf{d}=\mathbf{C}^{-1}\mathbf{f} \, . \tag{66}$$

Once the wave propagation coefficients are known, the shell displacements can be calculated using

$$u(x,r,t)=[-D_1\alpha \mathrm{J}_1(\alpha r)-D_2\alpha \mathrm{Y}_1(\alpha r)-D_3 \mathrm{i}k\mathrm{J}_1(\beta r)-D_4 \mathrm{i}k\mathrm{Y}_1(\beta r)]\exp(\mathrm{i}kx)\exp(-\mathrm{i}\omega t) \, , \tag{67}$$

and

$$w(x,r,t)=[D_1\mathrm{i}k\mathrm{J}_0(\alpha r)+D_2\mathrm{i}k\mathrm{Y}_0(\alpha r)+D_3\beta \mathrm{J}_0(\beta r)+G_4\beta \mathrm{Y}_0(\beta r)]\exp(\mathrm{i}kx)\exp(-\mathrm{i}\omega t) \, . \tag{68}$$

Once the displacements are known, the interior pressure field for this model can be calculated using

$$P_i(r)=\frac{-\omega^2\rho_i}{\gamma_i}\frac{\mathrm{J}_0(\gamma_i r)}{\mathrm{J}_1(\gamma_i a)}[-D_1\alpha \mathrm{J}_1(\alpha r)-D_2\alpha \mathrm{Y}_1(\alpha r)-D_3\mathrm{i}k\mathrm{J}_1(\beta r)-D_4\mathrm{i}k\mathrm{Y}_1(\beta r)] \, , \tag{69}$$

and the exterior pressure filed can be calculated using

$$P_o(r) = \frac{-\omega^2 \rho_o}{\gamma_o} \frac{\mathrm{H}_0^{(1)}(\gamma_o r)}{\mathrm{H}_1^{(1)}(\gamma_o a)} [-D_1 \alpha \mathrm{J}_1(\alpha r) - D_2 \alpha \mathrm{Y}_1(\alpha r) - D_3 ik \mathrm{J}_1(\beta r) - D_4 ik \mathrm{Y}_1(\beta r)] \ . \qquad (70)$$

Figure 4 is a plot of the transfer function of internal pressure at $r = 0$ divided by external forcing function in the radial direction versus wavenumber. Figure 5 is a plot of the transfer function of internal pressure at $r = 0$ divided by external forcing function in the longitudinal direction versus wavenumber. In both figures, the upper plot is the magnitude of the power expressed in the decibel scale and the lower plot is the phase angle expressed in degrees. The solid line is the transversely isotropic thick shell model developed in section 2, and the dots correspond to the isotropic thick shell model listed as equations (64) through (70). In this example, the transversely isotropic model was run with isotropic material properties, so the output of the transversely isotropic model should reasonably agree with the output of the isotropic model. Figures 4 and 5 were generated with the following parameters: frequency $f = 800$ Hz, shell density $\rho = 1200$ kg m^{-3}, radial Poisson's ratio due to longitudinal load $\upsilon_{xr} = 0.48$ (dimensionless), longitudinal Young's modulus $E_x = 3 \times 10^8$ N m^{-2}, radial Young's modulus $E_r = 3 \times 10^8$ N m^{-2}, longitudinal Poisson's ratio due to radial load $\upsilon_{rx} = 0.48$ (dimensionless), shear modulus $G_{xr} = 1.01 \times 10^8$ N m^{-2}, inner shell radius $a = 0.0762$ m, outer shell radius $b = 0.152$ m, inner fluid density $\rho_i = 800$ kg m^{-3}, inner fluid compressional wavespeed $c_i = 1300$ m s^{-1}, outer fluid density $\rho_o = 1000$ kg m^{-3}, and outer fluid compressional wavespeed $c_o = 1500$ m s^{-1}. Based on these values, the computed stiffness constants are $c_{11} = \lambda + 2\mu = 2.64 \times 10^9$ N m^{-2}, $c_{12} = \lambda = 2.43 \times 10^9$ N m^{-2}, $c_{13} = \lambda = 2.43 \times 10^9$ N m^{-2}, $c_{33} = \lambda + 2\mu = 2.64 \times 10^9$ N m^{-2} and $c_{44} = \mu = 1.01 \times 10^8$ N m^{-2}. Note that in figures 4 and 5, there is broad-based agreement between the thin shell model and the thick shell model.

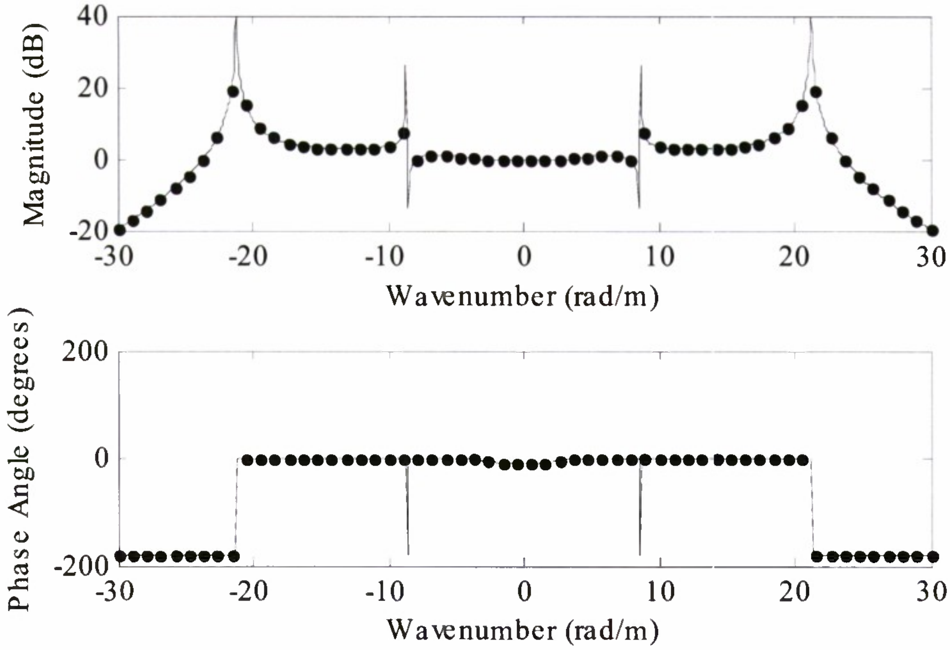

Figure 4. Transfer Function of Internal Pressure Divided by External Radial Excitation: Transversely Isotropic Thick Shell (——) and Isotropic Thick Shell (•)

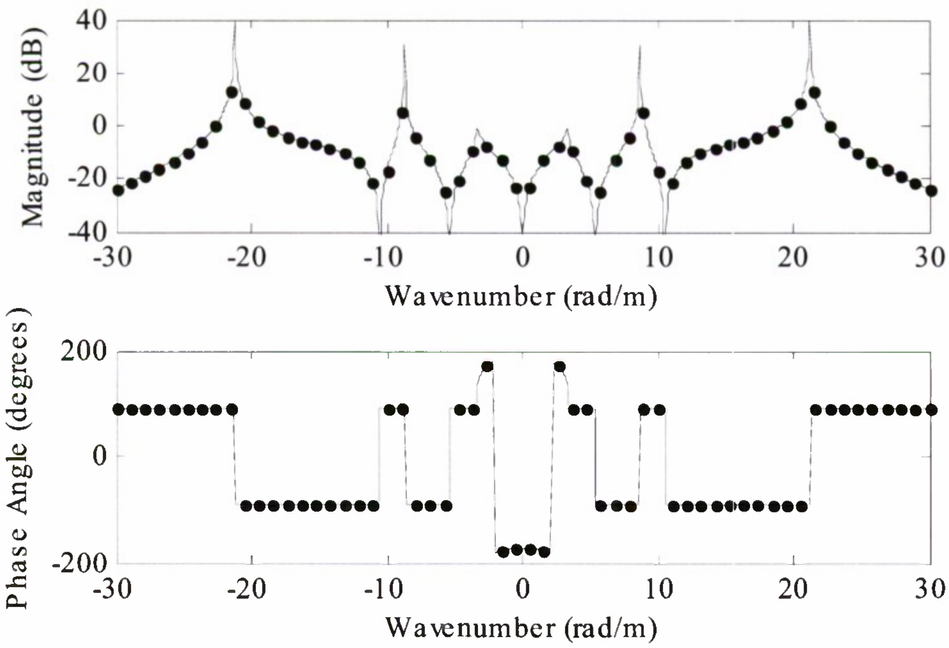

Figure 5. Transfer Function of Internal Pressure Divided by External Longitudinal Excitation: Transversely Isotropic Thick Shell (——) and Isotropic Thick Shell (•)

4. HIGH WAVENUMBER APPROXIMATION

Numerical simulations of this model reveal that at high wavenumbers the **A** matrix becomes ill-conditioned and algorithmically singular. To avoid this problem in any analysis, the outputs of the model, i.e., the transfer functions, are analyzed differently in two distinct regions—namely, where $|k| \le 5/a$ and where $|k| > 5/a$. In the region where $|k| > 5/a$, the model outputs are calculated in such a manner that they are continuous from $|k| \le 5/a$ to $|k| > 5/a$ and they are proportional to $1/k^4$. This is written in equation form as

$$\frac{P_i(r)}{P_e} \cong \begin{cases} \dfrac{P_i(r)}{P_e} & |k| \le \dfrac{5}{a} \\ \dfrac{A_0}{k^4} & |k| > \dfrac{5}{a} \end{cases}, \tag{71}$$

and

$$\frac{P_i(r)}{F_e} \cong \begin{cases} \dfrac{P_i(r)}{F_e} & |k| \le \dfrac{5}{a} \\ \dfrac{B_0}{k^4} & |k| > \dfrac{5}{a} \end{cases}, \tag{72}$$

where

$$A_0 = \left(\frac{5}{a}\right)^4 \left.\frac{P_i(r)}{P_e}\right|_{k=\frac{5}{a}}, \tag{73}$$

and

$$B_0 = \left(\frac{5}{a}\right)^4 \left.\frac{P_i(r)}{F_e}\right|_{k=\frac{5}{a}}. \tag{74}$$

This approximation ensures that the energy falloff past the flexural wave will occur in wavenumber at a rate that is observed in most shell models.

5. NUMERICAL EXAMPLE

A numerical example is now investigated using the transversely isotropic shell model derived in section 2. Figure 6 is an image of the magnitude of the transfer function of internal pressure at $r = 0$ divided by external forcing function in the radial direction versus frequency and wavenumber. This image is the magnitude of the power expressed in the decibel scale with the scale's range shown as a colorbar above the plot. Figure 7 shows constant frequency cuts of figure 6 at frequencies of 500, 1000, 1500, and 2000 Hz. Figure 8 is an image of the magnitude of the transfer function of internal pressure at $r = 0$ divided by external forcing function in the longitudinal direction versus frequency and wavenumber. This image is also the magnitude of the power expressed in the decibel scale with the scale's range shown as a colorbar above the plot. Figure 9 shows constant frequency cuts of figure 8 at frequencies of 500, 1000, 1500, and 2000 Hz. Figures 6 through 9 were generated with the following parameters: shell density ρ = 1200 kg m^{-3}, radial Poisson's ratio due to longitudinal load υ_{xr} = 0.48 (dimensionless), longitudinal Young's modulus E_x = 2 x 10^9(1-0.05i) N m^{-2}, radial Young's modulus E_r = 3 x 10^8(1-0.10i) N m^{-2}, longitudinal Poisson's ratio due to radial load υ_{rx} = 0.0722(1-0.0498i) (dimensionless), shear modulus G_{xr} = 6.76 x 10^8(1-0.05i) N m^{-2}, inner shell radius a = 0.0762 m, outer shell radius b = 0.1524 m, inner fluid density ρ_i = 800 kg m^{-3}, inner fluid compressional wavespeed c_i = 1300 m s^{-1}, outer fluid density ρ_o = 1000 kg m^{-3}, and outer fluid compressional wavespeed c_o = 1500 m s^{-1}. Based on these values, the computed stiffness constants are c_{11} = 3.15 x 10^8(1-0.103i) N m^{-2}, c_{12} = 3.46 x 10^7(1-0.156i) N m^{-2}, c_{13} = 1.68 x 10^8(1-0.108i) N m^{-2}, c_{33} = 2.16 x 10^9(1-0.0543i) N m^{-2}, and c_{44} = 6.76 x 10^8(1-0.05i) N m^{-2}. For this problem, the two validation models used in section 3 are not capable of modeling this configuration; thus, no comparison can be made with previously available solutions. The MATLAB code used to generate this (and the previous) example is included as appendix B.

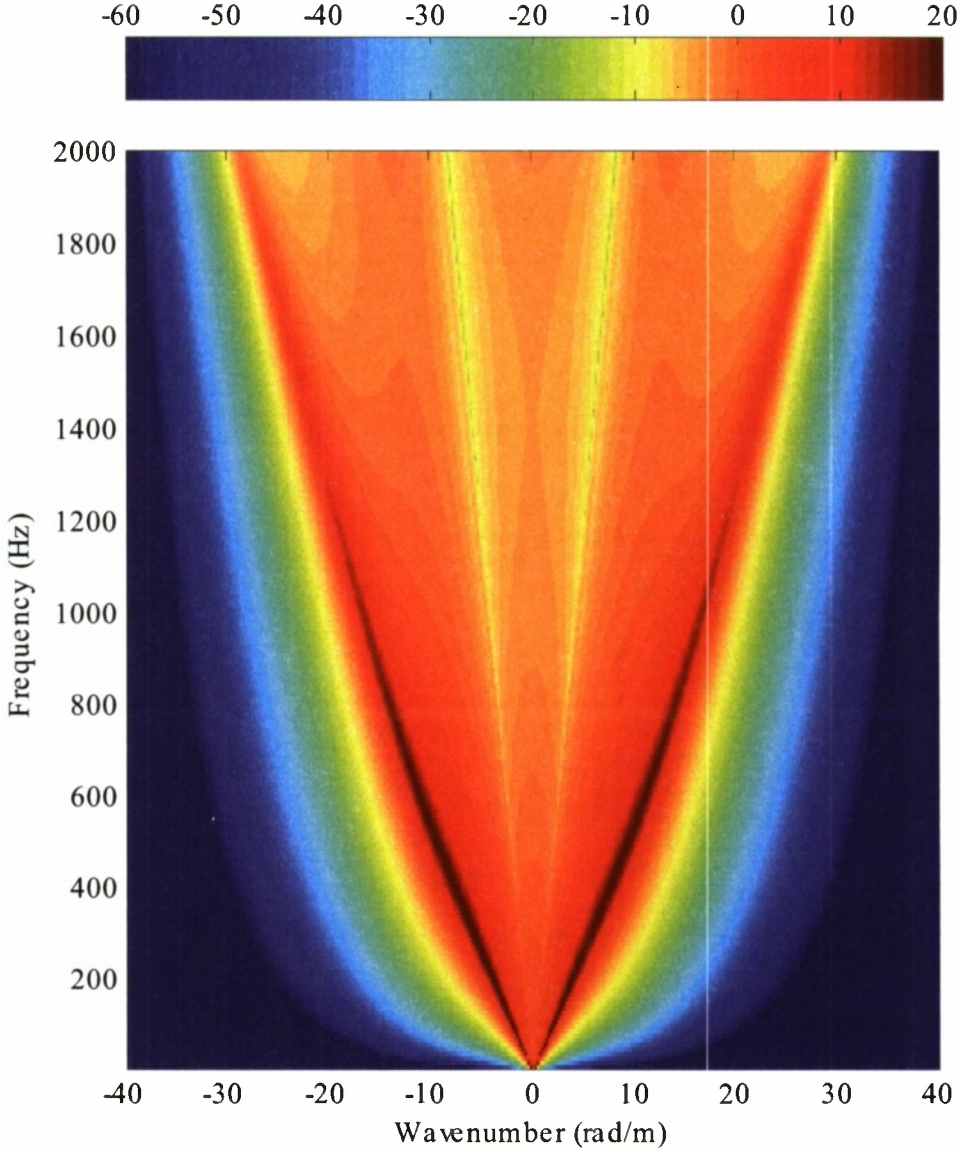

Figure 6. Transfer Function of Internal Pressure Divided by External Radial Excitation Versus Wavenumber and Frequency for Numerical Example

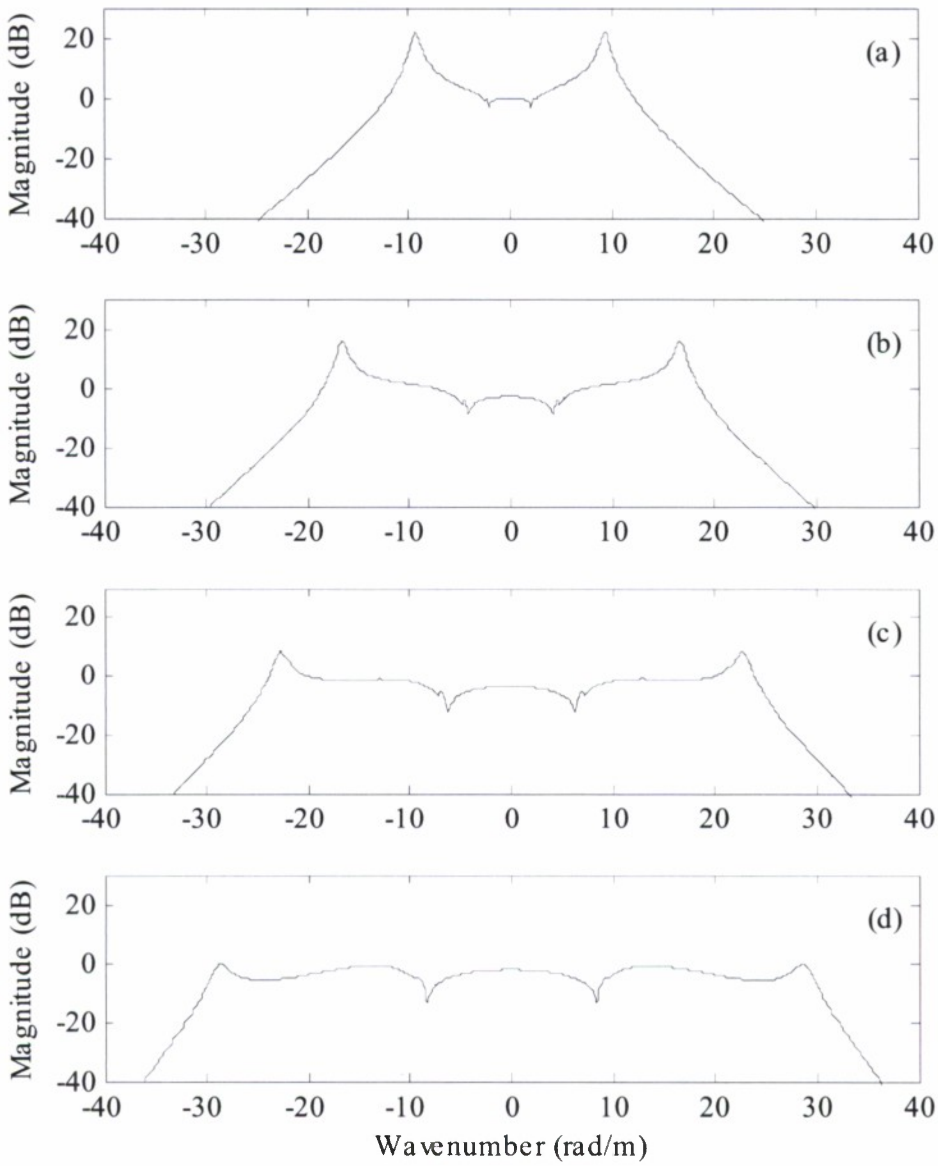

Figure 7. Transfer Function of Internal Pressure Divided by External Radial Excitation Versus Wavenumber for (a) 500 Hz, (b) 1000 Hz, (c) 1500 Hz, and (d) 2000 Hz

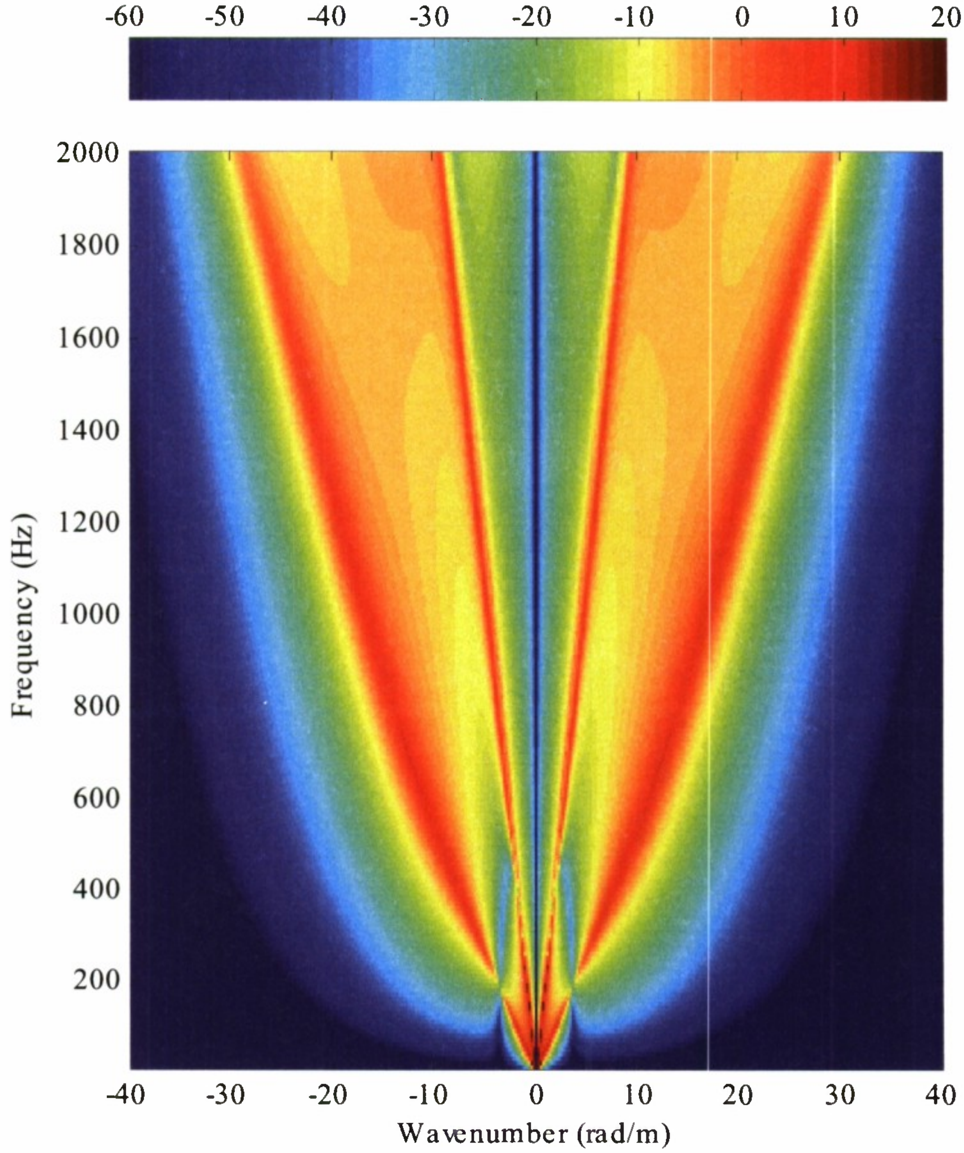

Figure 8. Transfer Function of Internal Pressure Divided by External Longitudinal Excitation Versus Wavenumber and Frequency for Numerical Example

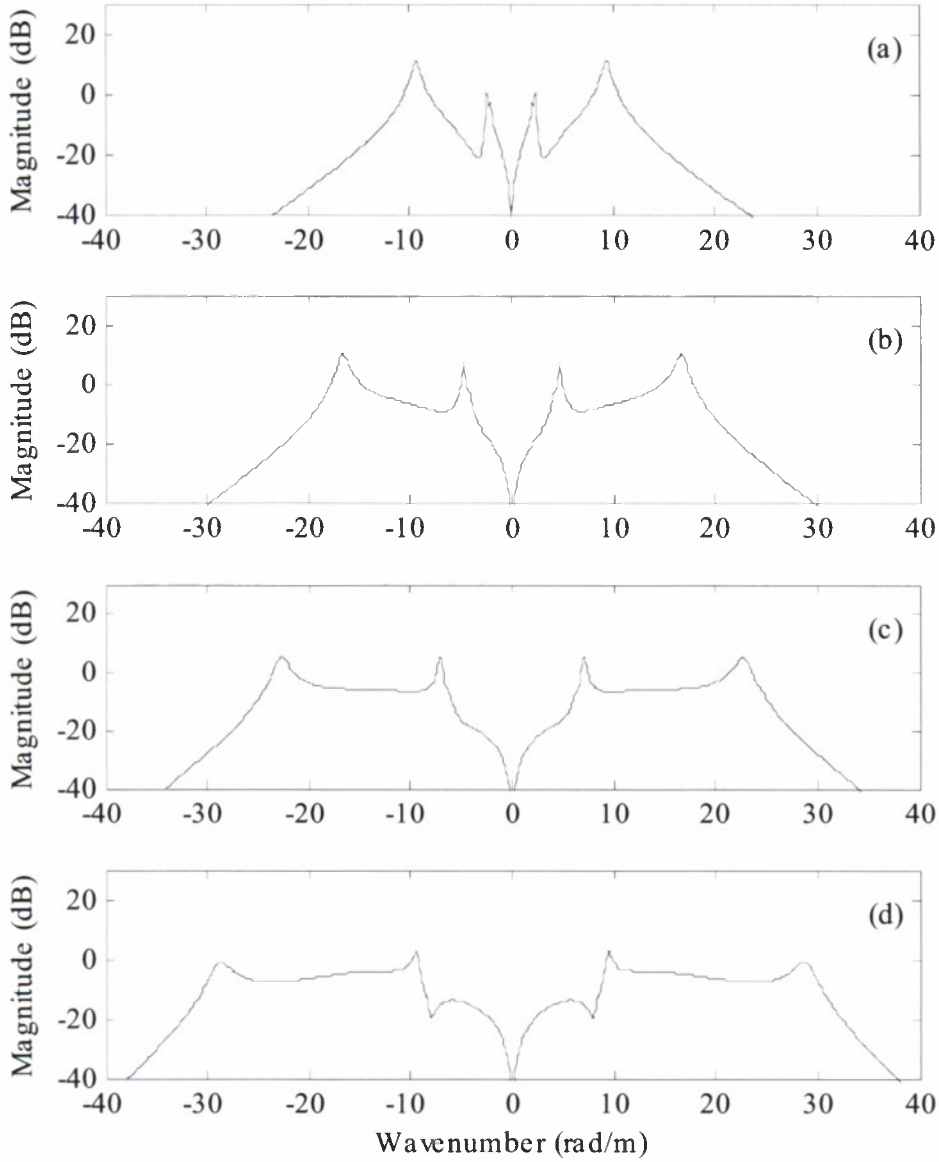

Figure 9. Transfer Function of Internal Pressure Divided by External Longitudinal Excitation Versus Wavenumber for (a) 500 Hz, (b) 1000 Hz, (c) 1500 Hz, and (d) 2000 Hz

6. SUMMARY

A model of a transversely isotropic thick shell with fluid loading on the inner and outer surfaces has been derived. This model is compared to two previously available models and is shown to be in agreement for the case where the shell is transversely isotropic and extremely thin and the case where the shell is isotropic and thick. A numerical example is given where the shell is transversely isotropic and thick. A calculation to bypass the high wavenumber instability that is typical of this class of problems is included. The MATLAB code used to generate the numerical examples is also included.

REFERENCES

1. A. E. H. Love, *A Treatise on the Mathematical Theory of Elasticity*, Dover Publications, New York, 1944.

2. H. Kraus, *Thin Elastic Shells*, John Wiley and Sons, New York, 1967.

3. I. Mirsky and G. Herrmann, "Nonaxially Symmetric Motions of Cylindrical Shells," *Journal of the Acoustical Society of America*, vol. 29, pp. 1116-1123, 1957.

4. I. Mirsky and G. Herrmann, "Axially Symmetric Motions of Thick Cylindrical Shells," *Journal of Applied Mechanics*, vol. 25, pp. 97-102, 1958.

5. D. C. Gazis, "Three-Dimensional Investigation of the Propagation of Waves in Hollow Circular Cylinders – I. Analytical Foundation," *Journal of the Acoustical Society of America*, vol. 31, pp. 568-573, 1959.

6. D. C. Gazis, "Three-Dimensional Investigation of the Propagation of Waves in Hollow Circular Cylinders – II. Numerical Results," *Journal of the Acoustical Society of America*, vol. 31, pp. 573-578, 1959.

7. R. R. Laverty, "Mechanics of Layered Cylindrical Elastic Waveguides," Ph.D. Dissertation, Colorado State University, 2001.

8. R. D. Fay, "Waves in Liquid-Filled Cylinders," *Journal of the Acoustical Society of America*, vol. 24, pp. 459-462, 1952.

9. M. S. Peloquin, "A Close-Form Dynamic Elasticity Solution to the Fluid/Structure Interaction Problem of a Two-Layer Infinite Viscoelastic Cylinder with Inner and Outer Fluid Loading Subject to Forced Harmonic Excitation," NUWC-NPT Technical Report 11,067, Naval Underwater Systems Center Division, Newport, RI, 29 December 1995.

10. H. Ding, W. Chen, and L. Zhang, *Elasticity of Transversely Isotropic Materials*, Springer, The Netherlands, 2006.

11. A. J. Hull, "A Non-Conforming Approximate Solution to a Specially Orthotropic Axisymmetric Thin Shell Subjected to a Harmonic Boundary Condition," *Journal of Sound and Vibration*, vol. 177, no. 5, pp. 611-621, 1994.

APPENDIX A
COEFFICIENTS OF MATRICES AND VECTORS

This appendix contains the coefficients of the matrices and vectors from the models developed in this report.

The entries of the **A** matrix from equation (53) are

$$a_{11} = (c_{11}\gamma_1 + ikc_{13}\xi_1)\mathrm{J}_0(\gamma_1 a) + \left(\frac{c_{12}-c_{11}}{a} + \frac{-\omega^2 \rho_i}{\gamma_i}\frac{\mathrm{J}_0(\gamma_i a)}{\mathrm{J}_1(\gamma_i a)}\right)\mathrm{J}_1(\gamma_1 a) \; , \tag{A-1}$$

$$a_{12} = (c_{11}\gamma_1 + ikc_{13}\xi_1)\mathrm{Y}_0(\gamma_1 a) + \left(\frac{c_{12}-c_{11}}{a} + \frac{-\omega^2 \rho_i}{\gamma_i}\frac{\mathrm{J}_0(\gamma_i a)}{\mathrm{J}_1(\gamma_i a)}\right)\mathrm{Y}_1(\gamma_1 a) \; , \tag{A-2}$$

$$a_{13} = (c_{11}\gamma_2 + ikc_{13}\xi_2)\mathrm{J}_0(\gamma_2 a) + \left(\frac{c_{12}-c_{11}}{a} + \frac{-\omega^2 \rho_i}{\gamma_i}\frac{\mathrm{J}_0(\gamma_i a)}{\mathrm{J}_1(\gamma_i a)}\right)\mathrm{J}_1(\gamma_2 a) \; , \tag{A-3}$$

$$a_{14} = (c_{11}\gamma_2 + ikc_{13}\xi_2)\mathrm{Y}_0(\gamma_2 a) + \left(\frac{c_{12}-c_{11}}{a} + \frac{-\omega^2 \rho_i}{\gamma_i}\frac{\mathrm{J}_0(\gamma_i a)}{\mathrm{J}_1(\gamma_i a)}\right)\mathrm{Y}_1(\gamma_2 a) \; , \tag{A-4}$$

$$a_{21} = c_{44}(ik - \gamma_1\xi_1)\mathrm{J}_1(\gamma_1 a) \; , \tag{A-5}$$

$$a_{22} = c_{44}(ik - \gamma_1\xi_1)\mathrm{Y}_1(\gamma_1 a) \; , \tag{A-6}$$

$$a_{23} = c_{44}(ik - \gamma_2\xi_2)\mathrm{J}_1(\gamma_2 a) \; , \tag{A-7}$$

$$a_{24} = c_{44}(ik - \gamma_2\xi_2)\mathrm{Y}_1(\gamma_2 a) \; , \tag{A-8}$$

$$a_{31} = (c_{11}\gamma_1 + ikc_{13}\xi_1)J_0(\gamma_1 b) + \left(\frac{c_{12} - c_{11}}{b} - \frac{-\omega^2 \rho_o}{\gamma_o}\frac{H_0^{(1)}(\gamma_o b)}{H_1^{(1)}(\gamma_o b)}\right)J_1(\gamma_1 b) \ , \tag{A-9}$$

$$a_{32} = (c_{11}\gamma_1 + ikc_{13}\xi_1)Y_0(\gamma_1 b) + \left(\frac{c_{12} - c_{11}}{b} - \frac{-\omega^2 \rho_o}{\gamma_o}\frac{H_0^{(1)}(\gamma_o b)}{H_1^{(1)}(\gamma_o b)}\right)Y_1(\gamma_1 b) \ , \tag{A-10}$$

$$a_{33} = (c_{11}\gamma_2 + ikc_{13}\xi_2)J_0(\gamma_2 b) + \left(\frac{c_{12} - c_{11}}{b} - \frac{-\omega^2 \rho_o}{\gamma_o}\frac{H_0^{(1)}(\gamma_o b)}{H_1^{(1)}(\gamma_o b)}\right)J_1(\gamma_2 b) \ , \tag{A-11}$$

$$a_{34} = (c_{11}\gamma_2 + ikc_{13}\xi_2)Y_0(\gamma_2 b) + \left(\frac{c_{12} - c_{11}}{b} - \frac{-\omega^2 \rho_o}{\gamma_o}\frac{H_0^{(1)}(\gamma_o b)}{H_1^{(1)}(\gamma_o b)}\right)Y_1(\gamma_2 b) \ , \tag{A-12}$$

$$a_{41} = c_{44}(ik - \gamma_1\xi_1)J_1(\gamma_1 b) \ , \tag{A-13}$$

$$a_{42} = c_{44}(ik - \gamma_1\xi_1)Y_1(\gamma_1 b) \ , \tag{A-14}$$

$$a_{43} = c_{44}(ik - \gamma_2\xi_2)J_1(\gamma_2 b) \ , \tag{A-15}$$

and

$$a_{44} = c_{44}(ik - \gamma_2\xi_2)Y_1(\gamma_2 b) \ . \tag{A-16}$$

The **g** vector from equation (53) is

$$\mathbf{g} = [G_1 \quad G_2 \quad G_3 \quad G_4]^T \ . \tag{A-17}$$

The **f** vector from equation (53) is

$$\mathbf{f} = \begin{bmatrix} 0 & 0 & -P_e & F_e \end{bmatrix}^{\mathrm{T}} \ . \tag{A-18}$$

The entries of the **B** matrix from equation (60) are

$$b_{11} = -\omega^2 \rho h + \frac{k^2 h E_x}{(1 - \upsilon_{rx}\upsilon_{xr})} \ , \tag{A-19}$$

$$b_{12} = \frac{\mathrm{i}kh\upsilon_{xr}E_r}{a(1 - \upsilon_{rx}\upsilon_{xr})} \ , \tag{A-20}$$

$$b_{21} = \frac{\mathrm{i}kh\upsilon_{rx}E_x}{a(1 - \upsilon_{rx}\upsilon_{xr})} \ , \tag{A-21}$$

and

$$b_{22} = -\omega^2 \rho h + \frac{k^4 h^3 E_x}{12(1 - \upsilon_{rx}\upsilon_{xr})} + \frac{hE_r}{a^2(1 - \upsilon_{rx}\upsilon_{xr})} + \frac{\omega^2 \rho_i}{\gamma_i} \frac{\mathrm{J}_0(\gamma_i a)}{\mathrm{J}_1(\gamma_i a)} + \frac{\omega^2 \rho_o}{\gamma_o} \frac{\mathrm{H}_0^{(1)}(\gamma_o a)}{\mathrm{H}_1^{(1)}(\gamma_o a)} \ . \tag{A-22}$$

The **u** vector from equation (60) is

$$\mathbf{u} = \begin{bmatrix} W & U \end{bmatrix}^{\mathrm{T}} \ . \tag{A-23}$$

The **p** vector from equation (60) is

$$\mathbf{p} = \begin{bmatrix} F_e & -P_e \end{bmatrix}^{\mathrm{T}} \ . \tag{A-24}$$

The entries of the **C** matrix from equation (65) are

$$c_{11} = \left[-(\lambda+2\mu)\alpha^2 - \lambda k^2\right] \mathrm{J}_0(\alpha a) + \left[\frac{2\mu\alpha}{a} - \alpha\left(\frac{-\omega^2\rho_i}{\gamma_i}\frac{\mathrm{J}_0(\gamma_i a)}{\mathrm{J}_1(\gamma_i a)}\right)\right] \mathrm{J}_1(\alpha a) \;, \tag{A-25}$$

$$c_{12} = \left[-(\lambda+2\mu)\alpha^2 - \lambda k^2\right] \mathrm{Y}_0(\alpha a) + \left[\frac{2\mu\alpha}{a} - \alpha\left(\frac{-\omega^2\rho_i}{\gamma_i}\frac{\mathrm{J}_0(\gamma_i a)}{\mathrm{J}_1(\gamma_i a)}\right)\right] \mathrm{Y}_1(\alpha a) \;, \tag{A-26}$$

$$c_{13} = -2\mathrm{i}\mu k\beta \, \mathrm{J}_0(\beta a) + \left[\frac{2\mathrm{i}\mu k}{a} - \mathrm{i}k\left(\frac{-\omega^2\rho_i}{\gamma_i}\frac{\mathrm{J}_0(\gamma_i a)}{\mathrm{J}_1(\gamma_i a)}\right)\right] \mathrm{J}_1(\beta a) \;, \tag{A-27}$$

$$c_{14} = -2\mathrm{i}\mu k\beta \, \mathrm{Y}_0(\beta a) + \left[\frac{2\mathrm{i}\mu k}{a} - \mathrm{i}k\left(\frac{-\omega^2\rho_i}{\gamma_i}\frac{\mathrm{J}_0(\gamma_i a)}{\mathrm{J}_1(\gamma_i a)}\right)\right] \mathrm{Y}_1(\beta a) \;, \tag{A-28}$$

$$c_{21} = -2\mathrm{i}\mu k\alpha \, \mathrm{J}_1(\alpha a) \;, \tag{A-29}$$

$$c_{22} = -2\mathrm{i}\mu k\alpha \, \mathrm{Y}_1(\alpha a) \;, \tag{A-30}$$

$$c_{23} = \mu(k^2 - \beta^2) \, \mathrm{J}_1(\beta a) \;, \tag{A-31}$$

$$c_{24} = \mu(k^2 - \beta^2) \, \mathrm{Y}_1(\beta a) \;, \tag{A-32}$$

$$c_{31} = \left[-(\lambda+2\mu)\alpha^2 - \lambda k^2\right] \mathrm{J}_0(\alpha b) + \left[\frac{2\mu\alpha}{b} + \alpha\left(\frac{-\omega^2\rho_o}{\gamma_o}\frac{\mathrm{H}_0^{(1)}(\gamma_o b)}{\mathrm{H}_1^{(1)}(\gamma_o b)}\right)\right] \mathrm{J}_1(\alpha b) \;, \tag{A-33}$$

$$c_{32} = \left[-(\lambda+2\mu)\alpha^2 - \lambda k^2\right] \mathrm{Y}_0(\alpha b) + \left[\frac{2\mu\alpha}{b} + \alpha\left(\frac{-\omega^2\rho_o}{\gamma_o}\frac{\mathrm{H}_0^{(1)}(\gamma_o b)}{\mathrm{H}_1^{(1)}(\gamma_o b)}\right)\right] \mathrm{Y}_1(\alpha b) \;, \tag{A-34}$$

$$c_{33} = -2\mathrm{i}\mu k\beta \, \mathrm{J}_0(\beta b) + \left[\frac{2\mathrm{i}\mu k}{b} + \mathrm{i}k \left(\frac{-\omega^2 \rho_o}{\gamma_o} \frac{\mathrm{H}_0^{(1)}(\gamma_o b)}{\mathrm{H}_1^{(1)}(\gamma_o b)} \right) \right] \mathrm{J}_1(\beta b) \; , \tag{A-35}$$

$$c_{34} = -2\mathrm{i}\mu k\beta \, \mathrm{Y}_0(\beta b) + \left[\frac{2\mathrm{i}\mu k}{b} + \mathrm{i}k \left(\frac{-\omega^2 \rho_o}{\gamma_o} \frac{\mathrm{H}_0^{(1)}(\gamma_o b)}{\mathrm{H}_1^{(1)}(\gamma_o b)} \right) \right] \mathrm{Y}_1(\beta b) \; , \tag{A-36}$$

$$c_{41} = -2\mathrm{i}\mu k\alpha \, \mathrm{J}_1(\alpha b) \; , \tag{A-37}$$

$$c_{42} = -2\mathrm{i}\mu k\alpha \, \mathrm{Y}_1(\alpha b) \; , \tag{A-38}$$

$$c_{43} = \mu(k^2 - \beta^2) \, \mathrm{J}_1(\beta b) \; , \tag{A-39}$$

and

$$c_{44} = \mu(k^2 - \beta^2) \, \mathrm{Y}_1(\beta b) \; . \tag{A-40}$$

In equations (A-25) through (A-40), the constants are as follows:

$$\alpha = (k_d^2 - k^2)^{1/2} = \left[\left(\frac{\omega}{c_d} \right)^2 - k^2 \right]^{1/2} , \tag{A-41}$$

and

$$\beta = (k_s^2 - k^2)^{1/2} = \left[\left(\frac{\omega}{c_s} \right)^2 - k^2 \right]^{1/2} , \tag{A-42}$$

where

$$c_d = \left(\frac{\lambda + 2\mu}{\rho} \right)^{1/2} , \tag{A-43}$$

and

$$c_s = \left(\frac{\mu}{\rho} \right)^{1/2} . \tag{A-44}$$

The relationship between the Lamé constants and the material properties is

$$\lambda = \frac{E\upsilon}{(1+\upsilon)(1-2\upsilon)} , \tag{A-45}$$

and

$$\mu = \frac{E}{2(1+\upsilon)} . \tag{A-46}$$

In equations (A-45) and (A-46), Young's modulus and Poisson's ratio can be along any axis because the material is isotropic.

APPENDIX B
MATLAB SUBROUTINE OF MODEL

```
%--ElasticShellTF---Elastic Shell Transfer Function
%
%---This program produces a model of the interior pressure
%    in a fluid filled shell when it is loaded on the exterior
%    by a normal and longitudinal force.  The shell has an
%    outer fluid and is transversly isotropic.  The behavior of
%    the shell is two-dimensional fully elastic.  Only the positve
%    wavenumber points are calculated because the model is symmetric
%    in wavenumber.
%
%--Written by Andrew J. Hull on 11/26/08
%
function [ PiDPo, PiDFo ] = ElasticShellTF
(freq,kmax,numpts,a,b,r,Ex,Er,nuxr,ro,roi,ci,roo,co)
%
%---Output Variables
%      PiDPo = Interior Pressure (at r) Divided by Exterior Normal Pressure
%      PiDFo = Interior Pressure (at r) Divided by Exterior Longituidnal Force
%
%---Input Variables
%      freq = Frequency (Hz)
%      kmax = Maximum wavenumber (rad/m)
%      numpts = Number of points in wavenumber
%      a = Inner shell radius (m)
%      b = Outer shell radius (m)
%      r = Hydrophone radius  (m)
%      Ex = Modulus in the axial direction (N/m^2)
%      Er = Modulus in the radial direction (N/m^2)
%      nuxr = Poisson's ratio of the matrix material (dimensionless)
%      ro = Density of the shell (kg/m^3)
%      roi = Density of the inner fluid (kg/m^3)
%      ci = Wavespeed of the inner fluid (m/s)
%      roo = Density of the outer fluid (kg/m^3)
%      co = Wavespeed of the outer fluid (m/s)
%
%-----------------------------------------------
%--Frequency in rad/s
w = 2 * pi * freq;
%--Build the wavenumber vector
kvec = linspace ( eps, kmax, numpts );
%--kahigh is the wavenumber cutoff where the high wavenumber
%   approximation is used in the analysis.  (This can be changed)
kahigh = 5.0;
%--Determine if the wavenumber vector has to be broken into low
%   and high regions
if ( a*kvec(end) > kahigh )
   startindexhigh = min ( find ( a*kvec > kahigh ) );
   klow  = kvec(1:1:startindexhigh-1);
   khigh = kvec(startindexhigh:1:end);
else
   klow = kvec;
end
%
%--Transversely isotropic material constants from physical constants
Gxr = Ex / ( 2 * ( 1 + nuxr ) );
nurx = nuxr * ( Er / Ex );
c11 = Er * (1-nurx*nuxr)   / ( (1+nurx) * (1-nurx-2*nurx*nuxr) );
```

```
c12 = Er * nurx * (1+nuxr) / ( (1+nurx) * (1-nurx-2*nurx*nuxr) );
c13 = Er * nuxr            /              (1-nurx-2*nurx*nuxr);
c33 = Er * nuxr * (1-nurx) / ( nurx     * (1-nurx-2*nurx*nuxr) );
c44 = Gxr;
%
%----------------------------------------------
%--Low wavenumber region ka < kahigh
b2 = c11*c44;
b1 = (c11*c33 - c13^2 - 2*c13*c44)*klow.^2 - (c44+c11)*ro*w^2;
b0 = ro^2*w^4 - ro*w^2*(c33+c44)*klow.^2 + c33*c44*klow.^4;
gamma1 = sqrt (  ( -b1 + sqrt ( b1.^2 - 4*b0*b2 ) ) / ( 2 * b2 )  );
gamma2 = sqrt (  ( -b1 - sqrt ( b1.^2 - 4*b0*b2 ) ) / ( 2 * b2 )  );
zeta1 = ( ro*w^2 - c11*gamma1.^2 - c44*klow.^2 ) ./ ( i*klow.*gamma1*( c13 +
c44 ) );
zeta2 = ( ro*w^2 - c11*gamma2.^2 - c44*klow.^2 ) ./ ( i*klow.*gamma2*( c13 +
c44 ) );
%
%--Inner fluid load
gammai = sqrt ( (w/ci)^2 - klow.^2 );
gammai = gammai + ( gammai == 0 )*eps;
fluidiload = ( (-w^2*roi) ./ gammai ) .* ( besselj(0,gammai*a) ./
besselj(1,gammai*a) );
%
%--Srr(a) = inner fluid load;
Amat11 = ( c11 * gamma1 + i * klow * c13 .* zeta1 )     .* besselj(0,gamma1*a)
+ ...
         ( ( c12 - c11 ) * ( 1 / a )  +  fluidiload )  .*
besselj(1,gamma1*a);
Amat12 = ( c11 * gamma1 + i * klow * c13 .* zeta1 )     .* bessely(0,gamma1*a)
+ ...
         ( ( c12 - c11 ) * ( 1 / a )  +  fluidiload )  .*
bessely(1,gamma1*a);
Amat13 = ( c11 * gamma2 + i * klow * c13 .* zeta2 )     .* besselj(0,gamma2*a)
+ ...
         ( ( c12 - c11 ) * ( 1 / a )  +  fluidiload )  .*
besselj(1,gamma2*a);
Amat14 = ( c11 * gamma2 + i * klow * c13 .* zeta2 )     .* bessely(0,gamma2*a)
+ ...
         ( ( c12 - c11 ) * ( 1 / a )  +  fluidiload )  .*
bessely(1,gamma2*a);
%
%--Srz(a) = 0;
Amat21 = c44 * ( i * klow - gamma1 .* zeta1 ) .* besselj(1,gamma1*a);
Amat22 = c44 * ( i * klow - gamma1 .* zeta1 ) .* bessely(1,gamma1*a);
Amat23 = c44 * ( i * klow - gamma2 .* zeta2 ) .* besselj(1,gamma2*a);
Amat24 = c44 * ( i * klow - gamma2 .* zeta2 ) .* bessely(1,gamma2*a);
%
%--Outer fluid load
gammao = sqrt ( (w/co)^2 - klow.^2 );
gammao = gammao + ( gammao == 0 )*eps;
fluidoload = ( (-w^2*roo) ./ gammao ) .* ( besselh(0,1,gammao*b) ./
besselh(1,1,gammao*b) );
%
%--Srr(b) = outer fluid load
Amat31 = ( c11 * gamma1 + i * klow * c13 .* zeta1 )     .* besselj(0,gamma1*b)
+ ...
         ( ( c12 - c11 ) * ( 1 / b )  -  fluidoload )  .*
besselj(1,gamma1*b);
Amat32 = ( c11 * gamma1 + i * klow * c13 .* zeta1 )     .* bessely(0,gamma1*b)
+ ...
         ( ( c12 - c11 ) * ( 1 / b )  -  fluidoload )  .*
bessely(1,gamma1*b);
Amat33 = ( c11 * gamma2 + i * klow * c13 .* zeta2 )     .* besselj(0,gamma2*b)
+ ...
```

```
         (  ( c12 - c11 ) * ( 1 / b )   -  fluidoload  ) .*
besselj(1,gamma2*b);
Amat34 = ( c11 * gamma2 + i * klow * c13 .* zeta2 )      .* bessely(0,gamma2*b)
+ ...
         (  ( c12 - c11 ) * ( 1 / b )   -  fluidoload  ) .*
bessely(1,gamma2*b);
%
%--srz(b)
Amat41 = c44 * ( i * klow - gamma1 .* zeta1 ) .* besselj(1,gamma1*b);
Amat42 = c44 * ( i * klow - gamma1 .* zeta1 ) .* bessely(1,gamma1*b);
Amat43 = c44 * ( i * klow - gamma2 .* zeta2 ) .* besselj(1,gamma2*b);
Amat44 = c44 * ( i * klow - gamma2 .* zeta2 ) .* bessely(1,gamma2*b);
%
%--Determinant of Amat
DetA = Amat11.*Amat22.*Amat33.*Amat44 - Amat11.*Amat22.*Amat34.*Amat43 + ...
      -Amat11.*Amat32.*Amat23.*Amat44 + Amat11.*Amat32.*Amat24.*Amat43 + ...
       Amat11.*Amat42.*Amat23.*Amat34 - Amat11.*Amat42.*Amat24.*Amat33 + ...
      -Amat21.*Amat12.*Amat33.*Amat44 + Amat21.*Amat12.*Amat34.*Amat43 + ...
       Amat21.*Amat32.*Amat13.*Amat44 - Amat21.*Amat32.*Amat14.*Amat43 + ...
      -Amat21.*Amat42.*Amat13.*Amat34 + Amat21.*Amat42.*Amat14.*Amat33 + ...
       Amat31.*Amat12.*Amat23.*Amat44 - Amat31.*Amat12.*Amat24.*Amat43 + ...
      -Amat31.*Amat22.*Amat13.*Amat44 + Amat31.*Amat22.*Amat14.*Amat43 + ...
       Amat31.*Amat42.*Amat13.*Amat24 - Amat31.*Amat42.*Amat14.*Amat23 + ...
      -Amat41.*Amat12.*Amat23.*Amat34 + Amat41.*Amat12.*Amat24.*Amat33 + ...
       Amat41.*Amat22.*Amat13.*Amat34 - Amat41.*Amat22.*Amat14.*Amat33 + ...
      -Amat41.*Amat32.*Amat13.*Amat24 + Amat41.*Amat32.*Amat14.*Amat23;
%
%--Protect against a zero divide
DetA = DetA + ( DetA == 0 )*eps;
%
%--Inverse terms of A (Not all terms are needed)
invA13 = (  Amat12.*Amat23.*Amat44 - Amat12.*Amat24.*Amat43 + ...
           -Amat22.*Amat13.*Amat44 + Amat22.*Amat14.*Amat43 + ...
            Amat42.*Amat13.*Amat24 - Amat42.*Amat14.*Amat23  ) ./ DetA;
%
invA14 = ( -Amat12.*Amat23.*Amat34 + Amat12.*Amat24.*Amat33 + ...
            Amat22.*Amat13.*Amat34 - Amat22.*Amat14.*Amat33 + ...
           -Amat32.*Amat13.*Amat24 + Amat32.*Amat14.*Amat23  ) ./ DetA;
%
%
invA23 = ( -Amat23.*Amat44.*Amat11 + Amat24.*Amat43.*Amat11 + ...
           -Amat41.*Amat13.*Amat24 + Amat41.*Amat14.*Amat23 + ...
            Amat21.*Amat13.*Amat44 - Amat21.*Amat14.*Amat43  ) ./ DetA;
%
invA24 = (  Amat23.*Amat34.*Amat11 - Amat24.*Amat33.*Amat11 + ...
            Amat31.*Amat13.*Amat24 - Amat31.*Amat14.*Amat23 + ...
           -Amat21.*Amat13.*Amat34 + Amat21.*Amat14.*Amat33  ) ./ DetA;
%
%
invA33 = (  Amat22.*Amat44.*Amat11 - Amat24.*Amat42.*Amat11 + ...
            Amat41.*Amat12.*Amat24 - Amat41.*Amat14.*Amat22 + ...
           -Amat21.*Amat12.*Amat44 + Amat21.*Amat14.*Amat42  ) ./ DetA;
%
invA34 = ( -Amat22.*Amat34.*Amat11 + Amat24.*Amat32.*Amat11 + ...
           -Amat31.*Amat12.*Amat24 + Amat31.*Amat14.*Amat22 + ...
            Amat21.*Amat12.*Amat34 - Amat21.*Amat14.*Amat32  ) ./ DetA;
%
%
invA43 = ( -Amat22.*Amat43.*Amat11 + Amat23.*Amat42.*Amat11 + ...
           -Amat41.*Amat12.*Amat23 + Amat41.*Amat13.*Amat22 + ...
            Amat21.*Amat12.*Amat43 - Amat21.*Amat13.*Amat42  ) ./ DetA;
%
invA44 = (  Amat22.*Amat33.*Amat11 - Amat23.*Amat32.*Amat11 + ...
            Amat31.*Amat12.*Amat23 - Amat31.*Amat13.*Amat22 + ...
```

```
          -Amat21.*Amat12.*Amat33 + Amat21.*Amat13.*Amat32  ) ./ DetA;
%
%--Shell displacement radial direction at a due to external radial pressure
ShellDispRadDPo = -invA13.*besselj(1,gamma1*a) - invA33.*besselj(1,gamma2*a) +
...
                  -invA23.*bessely(1,gamma1*a) - invA43.*bessely(1,gamma2*a);
%
%--Interior fluid pressure at r due to external radial pressure
PiDPo = ( (-w^2*roi) ./ gammai ) .* ShellDispRadDPo .* ( besselj(0,gammai*r)
./ besselj(1,gammai*a) );
%
%--Shell displacement radial direction at a due to external longituidnal force
ShellDispRadDFo = invA14.*besselj(1,gamma1*a) + invA34.*besselj(1,gamma2*a) +
...
                  invA24.*bessely(1,gamma1*a) + invA44.*bessely(1,gamma2*a);
%
%--Interior fluid pressure at r due to external longitudinal force
PiDFo = ( (-w^2*roi) ./ gammai ) .* ShellDispRadDFo .* ( besselj(0,gammai*r)
./ besselj(1,gammai*a) );
%
%-----------------------------------------------
%--High wavenumber region ka >= kahigh
if ( exist('khigh') == 1 )
   Azero = PiDPo(end) * (klow(end))^4;
   Bzero = PiDFo(end) * (klow(end))^4;
%
   PiDPohigh = Azero ./ ( khigh.^4 );
   PiDFohigh = Bzero ./ ( khigh.^4 );
%
   PiDPo( max(size(klow)+1) : max(size(kvec)) ) = PiDPohigh;
   PiDFo( max(size(klow)+1) : max(size(kvec)) ) = PiDFohigh;
%
end
%
%-----------------------------------------------
%--Populate the output vectors with the negative wavenumber response
PiDPo = [ fliplr(PiDPo(2:end)) PiDPo ];
PiDFo = [ fliplr(PiDFo(2:end)) PiDFo ];
%
end
%---------------------------------------------------------------
```

INITIAL DISTRIBUTION LIST

Addressee	No. of Copies
Office of Naval Research (ONR-321—M. Traweek)	2
Defense Technical Information Center	2
Center for Naval Analyses	1